33rd Annual International Conference of the IEEE EMBS
Boston, Massachusetts USA, August 30 - September 3, 2011

Automated High-Performance cIMT Measurement Techniques using Patented AtheroEdge™: A Screening and Home Monitoring System

Filippo Molinari, *Member, IEEE,* Kristen M. Meiburger, *Graduate Student Member, IEEE,* and Jasjit Suri, *Fellow AIMBE, Senior Member, IEEE*

Abstract—**The evaluation of the carotid artery wall is fundamental for the assessment of cardiovascular risk. This paper presents the general architecture of an automatic strategy, which segments the lumen-intima and media-adventitia borders, classified under a class of Patented AtheroEdge™ systems (Global Biomedical Technologies, Inc, CA, USA). Guidelines to produce accurate and repeatable measurements of the intima-media thickness are provided and the problem of the different distance metrics one can adopt is confronted. We compared the results of a completely automatic algorithm that we developed with those of a semi-automatic algorithm, and showed final segmentation results for both techniques. The overall rationale is to provide user-independent high-performance techniques suitable for screening and remote monitoring.**

I. Introduction

CARDIOVASCULAR diseases (CVDs) are an ever growing cause of death worldwide. Effective prevention has become a priority and is eased thanks to the fact that atherosclerosis, the earliest manifestation of the possible onset of a CVD, is a process that develops over a span of several decades before becoming clinically manifest.

A commonly used method for cardiovascular risk assessment is based on the acquisition of longitudinal 2D B-mode ultrasound images of the carotid artery (CA). In these images, the distal wall of the artery is clearly portrayed and the intima-media thickness (IMT), a reliable and widely used marker of the progression of atherosclerosis [1], [2], can be measured.

The IMT is, of today, still measured manually by the sonographer. However, it is evident how an automated measurement would bring numerous benefits to the cardiovascular risk screening process. In fact, an automated IMT measurement would reduce the average exam assessment duration, allowing more patients to be screened in the same time frame, and would remove subjectivity from the exam results. This would produce a rapid and accurate analysis of the carotid artery wall status.

These qualities can also be seen from a new perspective thanks to the development and use of telemedicine and healthcare informatics. In fact, a sonographer can easily screen many patients using a portable ultrasound device and not only electronically store the acquired image and the automatically computed IMT measurement, but also transmit the data to a medical specialist or to a database for a subsequent offline assessment.

This paper is meant to present the main qualities and steps of a generic completely automatic algorithm used for IMT measurement, a patented class of AtheroEdge™ system (Global Biomedical Technologies, Inc., CA, USA). The goal is to segment two interfaces that are represented in the longitudinal image of the artery: the lumen-intima boundary (LI) and the media-adventitia boundary (MA). The distance between the two interfaces is taken as an estimation of the IMT. The methods that can be adopted to increase the accuracy and repeatability of the algorithms' performances are discussed, along with potential difficulties that can be met. Finally, we present and discuss the performances of an automatic algorithm we previously developed and a semi-automatic algorithm developed by other authors [3].

II. Materials and Methods

A. Overview of the general architecture of an automatic algorithm for IMT measurement

In order to be considered completely automatic, the estimation of the IMT must be retrieved from the acquired B-mode ultrasound image as is. In order to achieve this, the entire process can be appropriately divided into different stages, which are presented here in detail.

1) Stage 0: Preprocessing. There are two important preprocessing steps: automatic cropping and speckle noise removal.

1.1) Automatic cropping: Raw ultrasound images which are acquired during an exam never contain solely the carotid artery in the image but rather present a surrounding black frame in which device headers and image/patient data are often portrayed (Fig. 1.A). This information is unnecessary for image processing, so to discard of it, the image must be automatically cropped. If the image is in a DICOM format, the automatic cropping process can be obtained thanks to the DICOM tags included in the header; if the image is not in a DICOM format, a gradient-based procedure can be adopted. The cropped image therefore contains exclusively the ultrasound data that is useful for IMT measurement (Fig. 1.B).

F. Molinari and K. M. Meiburger are with the Biolab, Department of Electronics, Politecnico di Torino, 10129 Torino, Italy; (e-mail: filippo.molinari@polito.it).

J. S. Suri is affiliated Research Professor with Department of Biomedical Engineering, Idaho State University, Pocatello, ID 83201 USA, and also a CTO of Global Biomedical Technologies, Inc., CA, USA.

978-1-4244-4122-8/11/$26.00 ©2011 IEEE

1.2) Speckle noise removal: The next important preprocessing step is attenuating speckle noise in the automatically cropped image. Speckle is a form of locally correlated multiplicative noise, which reduces the overall image quality by creating a “pixelated” effect. This proves to be detrimental not only to visual evaluation but also to numerical image processing algorithms [4], [5]. Previous studies by Loizou *et al* [6], [7] showed how a first-order local statistics filter (called *lsmv* by the authors) can efficiently attenuate speckle noise and gave the best performance in the specific case of ultrasound imaging.

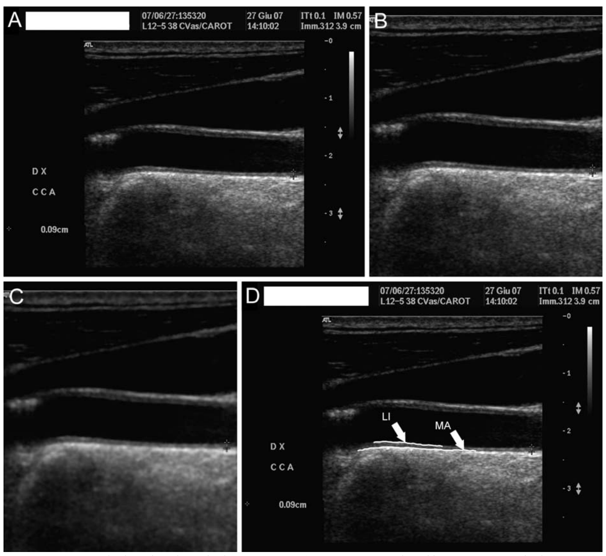

Fig. 1. A) Original sized image; B) Automatically cropped image; C) Despeckled image; D) Original image with LI and MA borders overlaid in white.

Therefore, we adopted this technique for speckle noise removal (Fig. 1.C).

2) Stage I: Recognition of the carotid artery (CA). Once the raw image has been appropriately preprocessed and before the segmentation of the LI and MA borders can be carried out, the carotid artery must be correctly located in the ultrasound image frame. This step allows the definition of a specifically reduced region-of-interest (ROI) containing the artery wall. This step directly influences the initialization of the segmentation stage (Stage II), and therefore also directly affects the final results.

The automatic delineation of the far adventitia layer (AD_F) in the image can be considered an appropriate approach for recognizing the CA in the image frame. In fact, the far adventitia layer is the outermost layer of the artery wall and is commonly portrayed in the B-mode ultrasound image as the brightest section of the image, allowing an easier identification. The ROI can then be defined by extending the AD_F profile upwards for a number of pixels that is found to be optimal with the pixel density of the considered image database.

3) Stage II: Segmentation of the LI and MA borders. Once the ROI has been defined, the true segmentation of the LI and MA borders can be initialized. Within the ROI of the grayscale image, therefore, various algorithms can be used to define the initial borders between the lumen and the intima layer and between the media and adventitia layers (Fig. 1.D). There are different approaches that can be undertaken to perform this stage. Some of the most prominent techniques include: (1) Edge tracking and gradient-based techniques; (2) Dynamic programming techniques; (3) Active contours (Snakes)-based segmentation; (4) Nakagami modeling; (5) Hough transform (HT); (6) Integrated approach; (7) Level set techniques.

4) Final stage: checks and refinement. Once the preliminary LI and MA borders have been extracted from the ultrasound image, there could be the need for some final checks and refinement processes. While each method may require different reconstruction techniques due to their differences, there are two global processes that we sustain to be fundamental for any method:

4.1) Anatomic (lumen) reference check: This check is important to avoid the potential error case in which the computed LI profile falls inside the lumen area. A good approach for this validation process is one in which the lumen region is modeled as a classification process with two classes. A bi-dimensional histogram (2DH) of the image can be subsequently obtained, representing in a joint manner both the mean value and the standard deviation of each pixel neighborhood. Previous studies [8] have demonstrated that the pixels belonging to the lumen generally fall into the first classes of the 2DH. A complete and exhaustive description of this specific process can be found in [9].

4.2) Spike removal: The preliminary LI and MA profiles can occasionally present spikes due to the fact that not every column of the image was correctly processed. The spike removal process can be based on the calculation of the first order derivative of the computed profile. The points of the profile that present a value over a specific cut-off limit can then be subsequently eliminated. A complete description of this specific process can be found in [9].

Once these four stages have been carried out, the final IMT value must then be measured. An initial raw IMT measurement can be obtained (IMT_{raw}) by simply calculating the distance between the LI and MA borders before the spike removal process. To increase the accuracy and repeatability of the measurement, however, spikes should be removed from the profiles as described previously. This gives forth another IMT value, $IMT_{NoSpikes}$. Two other steps can be implemented in order to increase the accuracy and the repeatability of the measurement even more. First of all, the profiles can be interpolated using a cubic spline data interpolation method (IMT_{interp}). Secondly, the profiles can be cut to a common support so that the distance calculated is not biased by the fact that one profile may be longer than the other (IMT_{cut}).

We present in this paper the results obtained for two different algorithms: (1) FOAM 2.0, a user-driven technique in which Stage I is done manually by the operator and Stage II, which is automated, is based on a first order absolute moment edge operator [3]; (2) CARES 3.0, a completely automated algorithm, is based on image feature extraction, fitting, and classification for Stage I and on the same first order absolute moment edge operator for Stage II [10]. We tested these algorithms on a database consisting of 300 images acquired at two different institutions. Table I presents the overall performances of these two algorithms.

B. Importance of the performance metric

With the continuous development of emerging techniques used for an automatic IMT measurement, a new problem that cannot be ignored also arises: the different performance metrics adopted to calculate the IMT. Some methods that are commonly used are the: Euclidean distance, Centerline distance, Polyline distance (PD) and Hausdorff distance (HD). For this paper, we adopted two different metrics for the calculation of the IMT: the Polyline distance, as described by Suri *et al* in 2000 [11] and the Hausdorff distance, which can be found in detail in [12]. Our rationale for choosing these metrics can be found in the Discussion section.

For a complete assessment of the algorithms' performances, it is fundamental to compare the computed IMT measurement with the IMT measurement obtained by manual operators. Ideally, ground truth (GT) profiles should be obtained by having different experts manually trace the LI and MA borders and then averaging the obtained profiles. A good example is using ImgTracer™ (GBTI, Inc., CA, USA). The ground truth IMT measurement is then obtained using the chosen distance metric. In this way, an IMT bias can be calculated as shown below.

$$IMT_{COMPUTED} = PD(computed_{LI}, computed_{MA}) \tag{1}$$

$$IMT_{GT} = PD(GT_{LI}, GT_{MA}) \tag{2}$$

$$\varepsilon^{IMT}_{COMPUTED} = IMT_{COMPUTED} - IMT_{GT} \tag{3}$$

The IMT bias should be calculated without an absolute value to give an idea of how much the algorithm underestimates and/or overestimates the IMT measurement. Table I shows the IMT biases computed for our image database.

For an overall assessment of the algorithm performance, the Figure of Merit (FoM) can be calculated, which is defined by the following formula:

$$FoM = \left(1 - \frac{\left|IMT_{COMPUTED} - IMT_{GT}\right|}{IMT_{GT}}\right) \cdot 100 \tag{4}$$

III. RESULTS

Figure 2 shows a gray-scale image cropped so as to contain the entire ROI with segmentation results (i.e., the LI and MA borders). The CARES 3.0 LI and MA borders are shown in the first column (Fig. 2.A) while the second column shows the results obtained using FOAM 2.0 (Fig. 2.B).

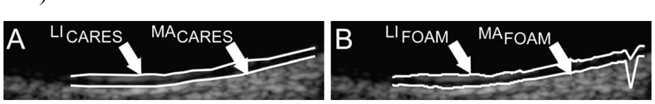

Fig. 2. A) Segmentation results for CARES; B) Segmentation results for FOAM.

Table I shows the overall performances for CARES 3.0 and FOAM 2.0. More specifically, it portrays the $\varepsilon^{IMT}_{COMPUTED}$ and the FoM calculated on our entire database. As described previously, we presented various ways to improve the raw IMT measurement in order to increase accuracy and repeatability. The columns show the various calculations for each progressive step in the IMT improvement process. As can be observed, the values obtained using the Polyline distance differ substantially from those obtained with the Hausdorff distance. This is due to its sensibility to the number of points in each boundary, as we explain in more detail in the Discussion section. Considering the Polyline distance, CARES 3.0 shows an improvement from -0.0658 ± 0.3080 mm (IMT_{raw}) to -0.0180 ± 0.3252 mm (IMT_{interp}), showing a Figure of Merit improvement from 92.17% to 97.85%. FOAM 2.0 shows an improvement from -0.0645 ± 0.3518 mm (IMT_{raw}) to -0.0018 ± 0.3718 mm (IMT_{interp}), showing a FoM improvement from 92.32% to 99.77%. It can be observed that the user-driven algorithm, FOAM 2.0, presents an overall more accurate result than our automatic algorithm, CARES 3.0. This result is not surprising since in FOAM 2.0, Stage I is done manually by an operator. This means that the ROI will contain the section of the artery wall presenting the least amount of noise. CARES 3.0, being completely automatic, cannot make such a distinction in the selection of the ROI. It can also be observed, however, that CARES 3.0 produces a more repeatable IMT measurement than FOAM 2.0, showing a lower standard deviation in all of the cases. Considering the Hausdorff distance, an initial observation portrays results that are not in complete accord with those obtained using PD. CARES 3.0 still shows a higher repeatability than FOAM 2.0, but its accuracy presents a worse value. This is again due to the HD sensibility to the number of points in each boundary. In fact, the FOAM 2.0 algorithm gives forth LI and MA borders which are made up of many more points when compared to the CARES 3.0 algorithm.

IV. DISCUSSION

We presented an overview of the architecture of a completely automatic algorithm used for IMT measurement in which the main steps, from preprocessing to final refinement, have been illustrated. The problem of the distance metric used to calculate the IMT was presented and we showed the results obtained using an image database of 300 images coming from two different institutions. One hundred images were acquired by the Neurology Division of Nicosia (Cyprus) and 200 from the Neurology Dept. of the Gradenigo Hospital of Torino (Italy).

A. Overall performances

Table I summarizes the performances of both CARES 3.0 and FOAM 2.0. It can be noted how the steps that we implemented in improving the IMT measurement can produce a more accurate PD measurement with a minimal difference in its repeatability. Our completely automated algorithm gave acceptable results compared to the semi-automatic algorithm, showing a general slightly lower accuracy but an improved repeatability. CARES 3.0 also presents the advantage of being completely automatic, a quality that is important for the screening process for cardiovascular risk.

B. Rationale for using the Polyline and Hausdorff distances

We chose to present two different distance metrics to illustrate how the final IMT measurement can vary substantially in relation to the distance metrics adopted. Table I clearly shows how the problem of automatic IMT measurement is not limited to the segmentation results of the LI and MA borders. We sustain therefore that it is of fundamental importance to use a distance metric that best presents the real distance between two different boundaries.

The Polyline distance, a calculation of the distance between the vertexes of one boundary and the segments of the other, seems to be a robust and reliable indicator of the distance between two boundaries. It presents the fundamental property of not depending on the number of points in either boundary. The Hausdorff distance, instead, is a calculation of the maximum distance of the minimum distances found between the vertexes of one boundary and the vertexes of the other. Two sets can be considered close if every point of either set is close to at least one other point in the other set. It is clear, therefore, how the HD is sensitive to the number of points in the boundaries, and not as reliable for IMT measurement but can be a useful tool for examining the farthest possible distance between two boundaries.

V. Conclusions

We presented a class of AtheroEdge™ system; a completely automated algorithm can be a great asset for cardiovascular risk screening. It can reduce human objectivity and allow a rapid processing of large databases. The general architecture can present four stages: preprocessing, recognition of the CA, segmentation of the LI and MA borders, and final checks and refinement. Once the LI and MA borders have been traced, the IMT can be measured. The distance metric adopted is of fundamental importance and must be chosen wisely, in order to best represent the distance between two boundaries.

A completely automatic algorithm that we developed presented results that were comparable to those of a semi-automatic algorithm. It was demonstrated how the raw IMT measurement can increase in accuracy by adopting steps and improving the raw LI and MA borders through spike removal, cubic spline interpolation, and cutting the profiles to a common support.

References

[1] P. J. Touboul, et al., "Mannheim carotid intima-media thickness consensus (2004-2006). An update on behalf of the Advisory Board of the 3rd and 4th Watching the Risk Symposium, 13th and 15th European Stroke Conferences, Mannheim Germany, 2004, and Brussels, Belgum, 2006," *Cerebrovasc Dis*, vol. 23, no. 1, pp. 75-80, 2007.

[2] P. J. Touboul et al., "Mannheim intima-media thickness consensus," *Cerebrovasc Dis,* vol. 18, no. 4, pp. 346-349, 2004.

[3] F. Faita, V. Gemignani, E. Bianchini, C. Giannarelli, L. Ghiadoni, and M. Demi, "Real-time measurement system for evaluation of the carotid intima-media thickness with a robust edge operator," *J Ultrasound Med,* vol. 27, pp. 1353-1361, 2008.

[4] C. B. Burckhardt, "Speckle in ultrasound B-mode scans," *IEEE Trans. Sonics Ultrason.,* vol. SU-25, no. 1, pp.1-6, 1978.

[5] R. F. Wagner, S. W. Smith, J. M. Sandrik, and H. Lopez, "Statistics of speckle in ultrasound B-scans," *IEEE Trans. Sonics Ultrason.,* vol. 30, pp. 156-163, 1983.

[6] C. P. Loizou, C. S. Pattichis, C. I. Christodoulou, R. S. H. Istepanian, M. Pantziaris, and A. Nicolaides, "Comparative evaluation of despeckle filtering in ultrasound imaging of the carotid artery," *Ultrasonics, Ferroelectrics and Frequency Control, IEEE Transactions on*, vol. 52, no. 10, pp. 1653-1669, 2005.

[7] C. P. Loizou, C. S. Pattichis, M. Pantziaris, T. Tyllis, and A. Nicolaides, "Quality evaluation of ultrasound imaging in the carotid artery based on normalization and speckle reduction filtering," *Med Biol Eng Comput*, vol. 44, no. 5, pp. 414-426, 2006.

[8] S. Delsanto, F. Molinari, P. Giustetto, W. Liboni, S. Badalamenti, and J. S. Suri, "Characterization of a completely user-independent algorithm for carotid artery segmentation in 2-D ultrasound images," *Instrumentation and Measurement, IEEE Transactions on,* vol. 56, pp. 1265-1274, 2007.

[9] F. Molinari, et al., "Completely automated multi-resolution edge snapper (CAMES) - A new technique for an accurate carotid ultrasound IMT measurement and its validation on a multi-institutional database," in *SPIE Medical Imaging Conference,* Lake Buena Vista (Orlando), FL, USA, 2011.

[10] F. Molinari, R. U. Acharya, G. Zeng, K.M. Meiburger and J. Suri, "CARES: Completely Automated Robust Edge Snapper for Carotid Ultrasound IMT measurement on a Multi-Institutional Database of 300 Images", *Med Biol Eng Comput*, (in press)

[11] J. S. Suri, R. M. Haralick, F. H. Sheehan, "Greedy algorithm for error correction in automatically produced boundaries from low contrast ventriculograms," *Pattern Analysis and Applications*, vol. 3, no. 1, pp. 39-60, 2000.

[12] Y. Zhen, S. Jasjit, S. Yajie, and R. Janer, "Four image interpolation techniques for ultrasound breast phantom data acquired using Fischer's full field digital mammography and ultrasound system (FFDMUS): a comparative approach." pp. II-1238-41.

TABLE I
OVERALL PERFORMANCES FOR CARES 3.0 AND FOAM 2.0

Distance Metric		Technique	IMT_{raw}	$IMT_{NoSpikes}$	IMT_{interp}	IMT_{cut}
PDM	ε^{IMT} [mm]	CARES 30.0	-0.066 ± 0.308	-0.046 ± 0.319	-0.018 ± 0.325	-0.035 ± 0.323
		FOAM 2.0	-0.064 ± 0.352	-0.039 ± 0.353	-0.002 ± 0.372	-0.035 ± 0.378
	FoM [%]	CARES 3.0	92.17	94.17	97.85	95.83
		FOAM 2.0	92.32	95.40	99.77	95.78
HDM	ε^{IMT} [mm]	CARES 3.0	-0.324 ± 0.887	-0.333 ± 0.891	-0.469 ± 0.816	-0.567 ± 0.799
		FOAM 2.0	0.033 ± 1.001	0.021 ± 0.994	0.124 ± 1.390	-0.147 ± 0.975
	FoM [%]	CARES 3.0	78.87	78.27	69.46	63.17
		FOAM 2.0	95.95	96.70	90.05	92.36

IMT_{raw} is the raw IMT measurement, $IMT_{NoSpikes}$ the IMT measurement obtained removing spikes, IMT_{interp} the measurement obtained interpolating the profiles, IMT_{cut} the measurement obtained cutting the profiles to a common support. ε^{IMT} is the IMT bias and FoM is the Figure of Merit.